

EMG-Force and EMG-Target Models During Force-Varying Bilateral Hand-Wrist Contraction in Able-Bodied and Limb-Absent Subjects

Ziling Zhu^{ID}, Member, IEEE, Carlos Martinez-Luna, Jianan Li, Member, IEEE, Benjamin E. McDonald, Chenyun Dai^{ID}, Associate Member, IEEE, Xinming Huang^{ID}, Senior Member, IEEE, Todd R. Farrell, and Edward A. Clancy^{ID}, Senior Member, IEEE

Abstract—System identification models relating forearm electromyogram (EMG) signals to phantom wrist radial-ulnar deviation force, pronation-supination moment and/or hand open-close force (EMG-force) are hampered by lack of supervised force/moment output signals in limb-absent subjects. In 12 able-bodied and 7 unilateral transradial limb-absent subjects, we studied three alternative supervised output sources in one degree of freedom (DoF) and 2-DoF target tracking tasks: (1) bilateral tracking with force feedback from the contralateral side (non-dominant for able-bodied/ sound for limb-absent subjects) with the contralateral force as the output, (2) bilateral tracking with force feedback from the contralateral side with the target as the output, and (3) dominant/limb-absent side unilateral target tracking *without* feedback and the target used as the output. “Best-case” EMG-force errors averaged $\sim 10\%$ of maximum voluntary contraction (MVC) when able-bodied subjects’ dominant limb produced unilateral force/moment with feedback. When either bilateral tracking source was used as the model output, statistically larger errors of 12–16 %MVC resulted. The no-feedback alternative produced errors of 25–30 %MVC, which was nearly half the tested force range of ± 30 %MVC. Therefore, the no-feedback model output was not acceptable. We found little performance variation between DoFs. Many subjects struggled to perform 2-DoF target tracking.

Index Terms—Amputee, biological system modeling, biomedical signal processing, electromyogram, electromyography, EMG-force.

I. INTRODUCTION

LI-MB-ABSENT subjects can generate motor commands that are communicated to remnant muscle tissue, which contracts and provides a measurable electromyogram (EMG) [1], [2]. This remnant muscle EMG is used to command myoelectric prostheses [3]. Proportional myoelectric control of one degree of freedom (DoF) prosthesis tasks has been available commercially for decades—including systems which support *sequential* switching between distinct DoFs [4]. So-called *seamless sequential* control has been achieved via pattern recognition [5] and recently commercialized. *Simultaneous, independent and proportional* control of multiple DoFs is mostly found in research systems and is primarily limited to 2-DoFs. Such control has typically been facilitated via multiple EMG sites [6] or advanced machine learning algorithms [7]. Our research described herein is applicable to simultaneous, independent and proportional 2-DoF hand-wrist prosthesis control.

In able-bodied subjects, biomedical signal processing and modelling methods have been used to map EMG to force [3], [8]–[12], and to mechanical impedance about a joint [13]–[17]. Historically, such modeling has a goal of improving myoelectric prosthesis control [3], [13], [17]. Numerous supervised system identification methods have been used to model the EMG-force (or, EMG-kinematics) relationship (see [9], [10] for reviews). All methods use an estimate of the EMG standard deviation ($EMG\sigma$, a.k.a. processed EMG) as input [18], [19], and may use other features extracted from the EMG signal, such as zero crossing rate, slope sign change rate and waveform length [5], [20]. Regression approaches have been common, with studies using standard (un-regularized) linear regression to fit the model [21], [22]. Recent work has used various forms or regularized regression, such as ridge [11], Moore-Penrose pseudo-inverse [11] and support

Manuscript received June 2, 2020; revised July 25, 2020 and November 4, 2020; accepted November 11, 2020. Date of publication November 16, 2020; date of current version January 29, 2021. This work supported in part by the U.S. Eunice Kennedy Shriver National Institute of Child Health and Human Development under Grant R42HD076519. (Corresponding author: Ziling Zhu.)

Ziling Zhu, Jianan Li, Xinming Huang, and Edward A. Clancy are with the Department of Electrical and Computer Engineering, Worcester Polytechnic Institute, Worcester, MA 01609 USA (e-mail: zzhu2@wpi.edu; jli6@wpi.edu; xhuang@wpi.edu; ted@wpi.edu).

Carlos Martinez-Luna, Benjamin E. McDonald, and Todd R. Farrell are with Liberating Technologies, Inc., Holliston, MA 01746 USA (e-mail: carlos.martinez@liberatingtech.com; benjamin.mcdonald@liberatingtech.com; todd.farrell@liberatingtech.com).

Chenyun Dai is with the Department of Electrical Engineering, Fudan University, Shanghai 200433, China (e-mail: chenyndai@fudan.edu.cn).

Digital Object Identifier 10.1109/TNSRE.2020.3038322

vector [23] regression approaches, to improve robustness of the model and reduce its error. Non-linear models have also been shown to reduce error somewhat, from implementations of the $EMG\sigma$ -force power law observation reported by Vredenburg and Rau [20], [24], to neural networks [25], [26], to parallel cascade structures [27], amongst many others. Some modeling approaches that require limited supervision are also emerging, including nonnegative matrix factorization [28], [29] and population-based assignment of dynamics [30], [31]. Of course, a classic approach with limited supervision is to insert dynamics in the form of a conventional linear lowpass filter (e.g., 2nd-order with cut-off frequency ~ 1.5 Hz) [32], [33]. Note that each of these less-supervised approaches still must calibrate a gain to each EMG channel.

A fundamental challenge for developing EMG-force models in limb-absent subjects is that end-effector force is not available as the output of supervised model training. As one alternative, EMG from remnant muscles of the absent limb are used to estimate the force (or kinematics) from the contralateral limb when performing bilateral symmetric (mirror) contractions [34]–[36]. This model is then used as the EMG-force relationship in the absent limb. Mirror-provided optical reflection of contralateral-side movement creates a visual illusion that builds awareness of phantom limb movement (and may relieve phantom limb pain) [1], [37]–[39]. Bilateral symmetric mirror tracking experiments on able-bodied subjects have found that relating dominant-limb EMG to contralateral hand position is slightly worse than relating it to dominant hand position [36]. However, experiments on amputees led to different results, as they had overall poorer performance than able-bodied subjects, but equal or better performance for some specific motions and their combinations [40]. The individual differences within limb-absent subjects was another important factor, as different kinds of limb-absence (i.e., congenital, traumatic), residual-limb length, or other conditions (e.g., neuron damage, contraction imbalance) may affect performance. Accordingly, some researchers prefer to individualize control methods for each specific subject [40].

An alternative approach is for limb-absent subjects to directly activate their phantom limb to track a target on a computer screen, then relate EMG to this target [23], [41]. This solution avoids the need for a physical feedback source (also applicable to those with bilateral limb-absence). However, this approach provides no physical measure of actual achieved remnant muscle force and always produces some amount of tracking error. For example, visual tracking incurs a pure reaction time delay between the target and the produced force (i.e., an average delay of 0.268 s [42]).

Our research extends prior EMG-force study in several manners. First, in able-bodied subjects, we compare and contrast different visual feedbacks within one study: dominant limb force, contralateral limb force with mirror feedback, and no force feedback. Second, in limb-absent subjects, the feedbacks studied were: contralateral¹ side using mirror feedback and no force feedback. Third, our novel methods

¹The term “contralateral” will be used to refer to the non-dominant side of able-bodied subjects and the sound side of limb-absent subjects.

TABLE I
TRANS-RADIAL LIMB-LOSS SUBJECT INFORMATION

| Sub. Num. | Sex | Age (years) | Type of Limb-Loss | Side | Time Limb Absent (years) | Residual Length (cm) | Circ. (cm) |
|-----------|-----|-------------|-------------------|------|--------------------------|----------------------|------------|
| 21 | F | 61 | Congenital | R | 61 | 5.5 | 19 |
| 22 | M | 27 | Congenital | L | 27 | 15 | 24 |
| 23 | M | 30 | Congenital | L | 30 | 13.5 | 25.5 |
| 25 | F | 49 | Traumatic | R | 32 | 10.5 | 22 |
| 26 | M | 54 | Traumatic | R | 37 | 14 | 20.8 |
| 27 | F | 58 | Traumatic | R | 33 | 13 | 19.6 |
| 28 | M | 36 | Congenital | L | 36 | 11 | 23 |

include instrumenting hand open-close (Opn-Cls) forces *as well as* wrist forces/moments, and doing so simultaneously on *both sides* of able-bodied subjects. We are not aware of any previous applicable studies that have simultaneously measured hand-wrist forces on *both* sides of able-bodied subjects. This instrumentation provided unique insights into evaluation of EMG-force models, including a direct measure as to how well forces in the contralateral limb are representative of forces in the dominant limb of able-bodied subjects. Our results have important implications for the calibration of myoelectric control algorithms, in particular the extent to which these measures can serve as surrogate supervised output sources for limb-absent subjects.

II. METHODS

A. Experimental Apparatus

Experimental data were collected from 12 able-bodied subjects (6 males, 6 females; aged 18–55 years) and 7 trans-radial unilateral limb-absent subjects (4 males, 3 females; aged 27–61 years; see Table I) at Worcester Polytechnic Institute (WPI) and approved by the WPI Institutional Review Board (IRB Protocol #17-155). All limb-absent subjects routinely use myoelectric-controlled upper-limb prostheses and all, except subject 27, were known to have previously participated as subjects in upper-limb myoelectric control studies. All subjects provided written informed consent. Able-bodied subjects had no deficits involving their upper limbs or vision and were right-hand dominant. Limb-absent subjects had no deficits involving their contralateral limb or vision, and the residual limb on the affected side was at least 5 cm in length with functional muscle contraction. One additional limb-absent subject was excluded due to neural damage on the limb-absent side.

Subjects were seated at the experimental apparatus (Fig. 1). The palm of each hand (sound side only for limb-absent subjects) was separately aligned and secured via Velcro straps to a thermo-formable plastic mold which was rigidly connected to a six-DoF load cell (MC3A-100 transducer, Gen 5 signal conditioner, AMTI, Watertown, MA) to measure radial-ulnar deviation (Rad-Uln) force along one force axis and pronation-supination (Pro-Sup) moment along one moment axis. Rad-Uln force was measured directly. However, this force is not produced at the axis origin of the load cell (which exists within the body of the load cell, approximately 6.3 cm from the



Fig. 1. Experimental apparatus. Subjects (limb-absent subject shown) sat in a chair with each able hand secured into force measurement devices, facing the computer screen which displayed a target and real-time force/moment feedback.

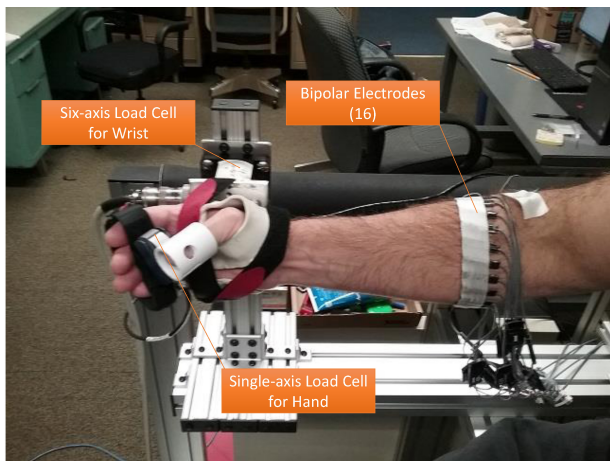


Fig. 2. Experimental apparatus at the hand-wrist. Each able hand was separately secured via Velcro to a thermo-formable plastic glove that was bolted to a six-axis load cell to measure the moment at the wrist. Fingers were secured to a single-axis load cell to measure hand grip force. Sixteen EMG electrodes were secured around the dominant/limb-absent forearm.

center of mass of the palm). Hence, Rad-Uln forces also produced an artifactual Pro-Sup moment. Thus, Pro-Sup moment was computed as the moment measured by the load cell, less the product of the Rad-Uln force times the 6.3 cm moment arm. To measure hand grip force during attempted hand Opn-Cls, each hand (sound side only for limb-absent subjects) additionally gripped a single-axis load cell (LCR-150 with DMD-465WB amplifier, Omega Engineering, Inc., Stamford, CT) while the thumb was secured via a rigid tube and, separately, the proximal aspects of the four fingers were secured by Velcro on the opposing side of the cell. The palms of the hands were oriented perpendicular to the plane of the floor, facing inwards; the wrists were relaxed in a neutral position; and the shoulders were in the anatomical position (Fig. 2).

During unilateral tasks (Fig. 3, Tasks 1 and 2), a computer-controlled target guided the subject to complete different experimental tasks via a blue arrowhead on the computer

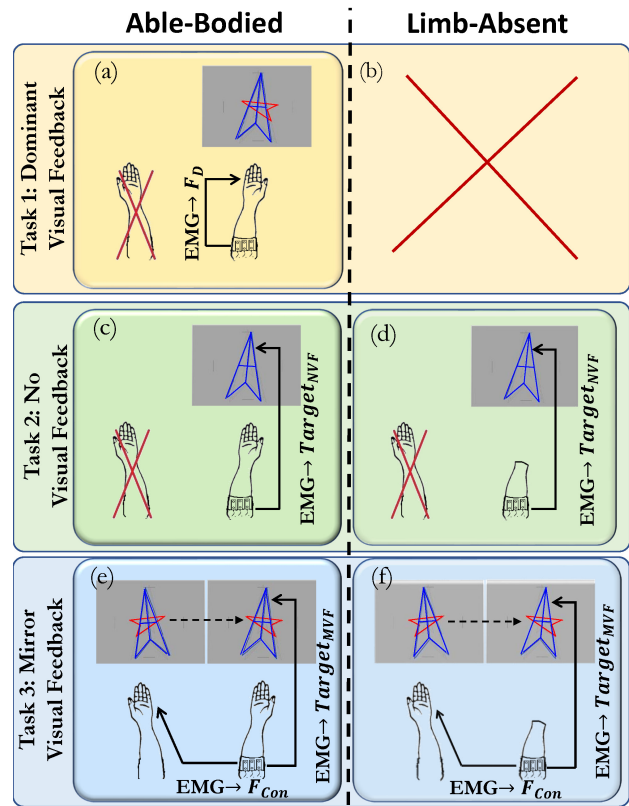


Fig. 3. Experiment Protocol. Blue arrowhead is target and red arrowhead is visual feedback. **a)** Task 1: able-bodied subjects tracked target with their dominant limb given real-time visual feedback of their dominant limb force (F_D); **c, d)** Task 2: subjects tracked the target with their dominant/limb-absent side with no visual feedback (NVF); **e, f)** Task 3: subjects tracked the target with both limbs given real-time feedback from their contralateral side and with mirror visual feedback (MVF).

screen in front of the subject, with up-down movement displaying wrist radial-ulnar deviation, rotation displaying Pro-Sup moment and arrowhead size displaying hand Opn-Cls force. (Wrist extension-flexion force was considered as an additional contraction dimension, but discarded due to the overall experimental protocol duration and its proximity to muscles used in hand Opn-Cls.) When desired, another red arrowhead displayed real-time force/moment feedback from both load cells on the dominant/affected or contralateral side, depending on the task being performed. During bilateral tasks (Fig. 3, Task 3), these displays were mirrored in two display panels on the screen.

One array of 16 bipolar EMG electrodes was secured to a subject's forearm (dominant side for able-bodied subjects, affected side for limb-absent subjects). Electrode gel was applied to a subject's forearm and the electrodes were equally spaced about its circumference, with the midpoints of the bipolar contacts placed 5 cm distal to the elbow crease. Each electrode pair consisted of 5 mm diameter, stainless steel, hemispherical contacts separated 1 cm edge-to-edge, oriented along the forearm's long axis. A reference electrode was gelled and secured on the forearm, just proximal to the active electrodes. Each bipolar EMG signal was differentially amplified (Liberating Technologies, Inc. BE328 amplifier;

30–500 Hz pass band, CMRR > 100 dB over the pass band) and then selectable gain was applied. All EMG channels and load cell signals were sampled at 2048 Hz with 16-bit resolution, and target movement was recorded at 800 Hz.

B. Experimental Protocol

All trials were constant-posture. To prevent cumulative fatigue, the interval between trials was at least two minutes. All limb-absent subjects were offered mirror-box training, using methods designed by a consulting occupational therapist, before tracking trials to help build a better sense of muscle contraction for the different tasks.

1) *MVC Trials*: After a warm-up period during which each task was introduced, able-bodied subjects performed bilateral maximum voluntary contraction (MVC) trials for each of wrist radial and ulnar deviation, wrist pronation and supination, and hand close and open. Limb-absent subjects only performed MVC trials for the sound side. All subjects took 2–3 seconds to ramp up to their MVC effort and then maintained this effort for 2–3 seconds. The plateau force/moment during the maintained period was recorded as the MVC. Lastly, rest trials with all muscles fully relaxed were recorded for EMG noise level evaluation.

2) *Force-Varying Target Tracking Trials*: Next, subjects performed force-varying target tracking Tasks 1, 2 and 3 (explained below) separately for 1-DoF Rad-Uln, Pro-Sup and Opn-Cls; and 2-DoF Rad-Uln & Opn-Cls and, separately, Pro-Sup & Opn-Cls. The 2-DoF tasks always included Opn-Cls, as this function is fundamental to a hand-wrist prosthesis. Only the utilized motions were enabled for visualization in the screen display (i.e., the remaining DoFs were locked out). The target was a 0.75 Hz band-limited, white and uniform random process [16] between $\pm 30\%$ MVC (independently generated for each DoF) corresponding to the utilized task. This bandwidth was the widest for which subjects could maintain target tracking for these tasks during preliminary testing. The order of presentation of DoFs, unilateral/bilateral and visual feedback condition (see below) was randomized and the subjects were told which side was controlling the feedback. Each trial was 40 s in duration and conducted twice per task. Before each trial, subjects were instructed about the range of target movements and allowed practice until they were comfortable. Unilateral and bilateral tasks were completed as described subsequently.

Task 1—Tracking with Dominant-Limb Force Feedback (Fig. 3a): Only able-bodied subjects performed these force-varying tracking tasks, using their dominant limb (with EMG electrodes). Feedback of dominant force/moment was provided for target tracking. The contralateral limb was fully at rest and not secured to the load cells. Off-line, EMG (which was acquired only from the dominant side) was related to force/moment on the dominant side. This task provides the best-case scenario for supervised learning of EMG-force models since EMG is recorded directly from the muscles producing the measured force/moment and, thus, represents the benchmark. Limb-absent subjects did not complete this task.

Task 2—Unilateral Tracking with No Visual Feedback (Fig. 3c, d): Able-bodied subjects used their dominant limb (with electrodes) to track the target, with no real-time feedback provided. Only the target was shown on the screen. Limb-absent subjects used the limb-absent side (the only side with electrodes) to track the target, with no real-time feedback provided. For all subjects, the contralateral limb was fully at rest (not secured to the load cells). Off-line, EMG was related to the target. This task represents the no-feedback condition in which a dominant/limb-absent side model is built without feedback.

Task 3—Bilateral Tracking with Mirror Visual Feedback (Fig. 3e, f): Able-bodied subjects used both limbs to simultaneously track the target. Limb-absent subjects used their sound and phantom limbs to simultaneously track the target. For all subjects, feedback consisted only of the force produced by the contralateral-side limb. This force and its mirror force were simultaneously displayed, producing mirror visual feedback. Offline, EMG was related to contralateral-side force/moment. This task represents use of the force/moment in the contralateral side in order to build the dominant/limb-absent side model. We also related EMG to the target, for comparison.

C. Methods of Analysis

1) *Data Pre-Processing*: Data processing was performed in MATLAB 2018b (Mathworks, Inc., Natick, MA). All filters were implemented using the two-pass, zero-phase method, thus their effective filter orders are twice those listed herein. The forces/moments (Rad-Uln, Opn-Cls, Pro-Sup) were each lowpass filtered ($f_c = 16$ Hz; Chebyshev Type I filter, ninth-order, 0.05 dB peak-to-peak passband ripple) and then downsampled from 2048 Hz to 40.96 Hz. The wrist Rad-Uln data were normalized by $(|MVC_{Rad}| + |MVC_{Uln}|)/2$, and similar normalization was applied to the Pro-Sup and Opn-Cls data. All target data were identically lowpass filtered, then resampled to 40.96 Hz.

For each of the 16 EMG channels in a trial, an estimate of time-varying EMG standard deviation ($EMG\sigma[m]$, where m was the decimated discrete-time sample index) was computed. The raw EMG were highpass filtered ($f_c = 15$ Hz, fifth-order Butterworth filter) to remove motion artifact, then notch filtered (second-order IIR filter at 60 Hz, notch bandwidth of 1 Hz), rectified, lowpass filtered ($f_c = 16$ Hz, as above) and finally downsampled to 40.96 Hz. Note that additional lowpass filtering, typically with $f_c \leq 1$ Hz, is optimized to each subject via the $EMG\sigma$ -force/target model [33]. Prior to further analysis, the initial and final 1 s of all signals were removed to avoid filter startup transients.

2) *Latency Between Forces/Moments and the Target*: For each able-bodied subject and DoF, we computed the cross-correlation coefficient function to estimate the latency between subject force/moment and the target [43]. For 2-DoF tasks, latency estimates were made independently for each DoF. The time location of the maximum of the cross-correlation coefficient function indicated the time delay (latency) ($\tau = k/F_s$, where k is the number of samples, F_s is the sampling frequency) at which the force/moment

and the target were best aligned. The corresponding maximum cross-correlation coefficient function value (ρ) is a measure of the linear association of the target tracking, after accounting for the latency. It is invariant to gain and, as such, is a measure of *timing* accuracy in tracking. As the force will lag behind target movement due to the subject's reaction time, we only searched for the maximum ρ between a delay τ of 0 to 1 s. Note that our pre-processing of the force/moment data did not bias the latency estimates, since pre-processing filters were implemented with zero phase.

3) *Dynamic EMG σ -Force/Target Modeling*: When EMG σ [m] was related to force (EMG-force), or when EMG was related directly to the arrowhead target (EMG-target), during 1-DoF trials, a linear, dynamic, finite impulse response relation was used, of the form:

$$F[m] = \sum_{q=0}^Q \sum_{e=1}^E c_{e,q} \text{EMG}\sigma_e[m - q - k],$$

where F was the force/target, m was the decimated discrete-time sample index, q and e were integer indexes, $Q = 20$ was the order of the linear dynamic model, $E = 16$ was the number of electrodes used in the fit, and $c_{e,q}$ were the fit coefficients [44]. Latency (k ; in samples) was assigned to zero for EMG-force models (we observed that sufficient latency was provided by the frequency-dependent phase response of the linear models). For EMG-target models of able-bodied subjects, latency was taken from the same trial as the model fit, as this value was assumed to be most accurate; for limb-absent subjects (wherein latency cannot be measured on the limb-absent side), the latency used was the average latency from able-bodied subject trials from the same task and DoF. Fit coefficients were estimated via the linear least squares pseudo-inverse method, in which singular values of the design matrix were removed if the ratio of that singular value to the largest was less than a tolerance value ($Tol = 0.1$, based on previous study [11], [20]). We chose this modeling method for its robustness, simplicity and because linear models capture most of the EMG-force/target relationship. In this manner, we could maintain our focus on the different feedback mechanisms.

Each task consisted of two trials. The first trial was used for coefficient training and the second for testing. Then, the training and testing trials were flipped for two-fold cross-validation and the average of the two RMS errors (RMSEs) reported. All RMSEs were in %MVC (normalized force/moment).

For 2-DoF trials, two EMG σ -force/target models were fit, one per DoF (each with its own coefficients). In this manner, each EMG channel contributed to each DoF. Again, one trial was used for training and one for testing, with two-fold cross-validation.

4) *EMG-Force, EMG-Target Models Studied*: For each experimental task, both 1- and 2-DoF trials had been performed. Thus, both 1- and 2-DoF EMG-force/target models were studied, respectively. From the Task 1 data, EMG σ was related to force in the dominant arm. These data were only available from the able-bodied subjects and represented the reference ("best-case") task. From the Task 2 data in which there was

TABLE II
ABLE-BODIED SUBJECTS, TRACKING LATENCY BETWEEN ACTUAL FORCE/MOMENT AND TARGET, FOR EACH DOF (MS)

| 1-DoF: | Rad-Uln | Pro-Sup | Opn-Cls |
|------------------|---------|---------|---------|
| Task 1, Dominant | 268±46 | 300±68 | 330±75 |
| Task 2, Dominant | 274±100 | 240±79 | 234±73 |
| Task 3, Dominant | 278±53 | 349±144 | 353±88 |
| Contralateral | 293±54 | 349±98 | 367±102 |

| 2-DoF: | Rad-Uln | Opn-Cls | Pro-Sup | Opn-Cls |
|------------------|---------|---------|---------|---------|
| Task 1, Dominant | 242±37 | 491±90 | 289±38 | 485±100 |
| Task 2, Dominant | 431±171 | 458±192 | 263±72 | 509±189 |
| Task 3, Dominant | 270±30 | 524±94 | 325±51 | 528±94 |
| Contralateral | 297±40 | 523±120 | 364±49 | 535±92 |

no visual feedback, EMG σ only was related to the target for all subjects. This analysis represents building models when no feedback is available during training (e.g., when building EMG-force style prosthesis control models for limb-absent subjects). From the Task 3 data that used mirror visual feedback, EMG σ was related to contralateral force (representing use of forces from the sound side to train models in unilateral limb-absent subjects); and EMG σ was related to the target for all subjects (for comparison to results from Task 2). Again, the average RMSEs from two-fold cross-validated results is reported.

D. Statistics

Our primary evaluation metrics were latency between forces/moments and the target, and maximum cross correlation coefficient/RMSE between measured/EMG-estimated forces/moments. Unless noted otherwise, performance differences were evaluated using repeated measures analysis of variance (RANOVA) in SPSS 22, using a significance level of $p = 0.05$. Prior to RANOVA, the degree of sphericity (ϵ) was used to adjust the degrees of freedom by either the method of Greenhouse-Geisser ($\epsilon < 0.75$) or the method of Huynh-Feldt ($0.75 < \epsilon < 1$). Unless stated otherwise, no interactions were found. Pairwise comparisons (*post hoc* or stand-alone) were conducted using paired *t*-tests with Bonferroni correction. We statistically analyzed 1-DoF tasks separately from 2-DoF tasks.

III. RESULTS

A. Latencies Between Force/Moment and Target

Table II shows the mean \pm std. dev. latencies between force/moment and target for each experimental task, for the able-bodied subjects. RMSE between force/moment and target was compared pairwise with vs. without latency adjustment. Pooling all conditions [288 1-DoF trials (12 subjects \times 4 feedback types \times 3 DoFs \times 2 sets) and 384 2-DoF trials (12 subjects \times 4 feedback types \times 2 DoF pairs \times 2 errors per DoF pair \times 2 sets)], the latency adjusted error was smaller (in 658 of 672 pairs) by an average of 4.60 ± 2.91 %MVC, which was statistically significant ($p < 10^{-6}$, paired sign test). This result formed the basis for our step in the Methods section to latency-adjust all EMG-target models.

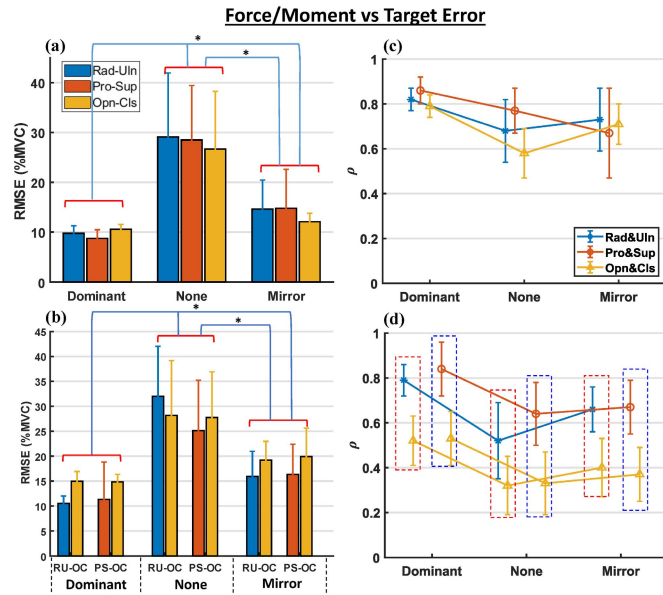


Fig. 4. Mean + std. dev. errors between dominant limb force/moment and target for able-bodied subjects, after adjusting for time latency. Statistically significant differences between feedback types indicated with “*”. RMSE (left) with different feedback conditions [dominant (Task 1), none (Task 2) and mirror (Task 3)] as a function of DoF for 1-DoF tasks (top) and as a function of DoF pairs for 2-DoF tasks (bottom). Maximum cross-correlation coefficients (ρ) shown at right. Dash-line boxes in (d) group DoF pairs.

B. RMSE, Dominant Force vs. Target, Able-Bodied Subjects

Before reporting EMG-force and EMG-target performance (see subsequent sub-sections), we describe the ability of able-bodied subjects to track the random target in Tasks 1–3. Fig. 4 shows summary RMSE and ρ of dominant limb force in able-bodied subjects vs. target for the different feedback conditions (i.e., tasks), after adjusting for time latency. RMSE measures tracking error, while ρ provides an error measure that is invariant to gain (and provides our latency values).

In 1-DoF tasks, a two-way RANOVA of RMSE with the factors feedback (dominant, none, mirror) and DoF (Rad-Uln, Pro-Sup, Opn-Cls) found only feedback as significant [$F(1.1, 12.6) = 42, p_{GG} = 10^{-5}$]. Pairwise comparison found RMSE in dominant feedback was significantly lower than none ($p = 10^{-4}$) and mirror ($p = 0.002$), and mirror had significantly lower error than none ($p = 10^{-4}$).

In 2-DoF tasks, a three-way RANOVA for tracking RMSE with the factors of feedback (dominant, none, mirror), DoF pair (Rad-Uln & Opn-Cls or Pro-Sup & Opn-Cls) and motion-within-DoF (wrist Rad vs. Uln, or Pro vs. Sup; or hand Opn vs. Cls) found only feedback was significant [$F(1.2, 13.0) = 40, p_{GG} = 10^{-5}$]. Pairwise comparison found RMSE in dominant feedback was significantly lower than none ($p = 10^{-4}$) and mirror ($p = 10^{-4}$), and RMSE in mirror was significantly lower than none ($p = 0.001$). In both 1-DoF and 2-DoF tasks, the average error when using no feedback is nearly half the contraction range of ± 30 %MVC, which seems unacceptable.

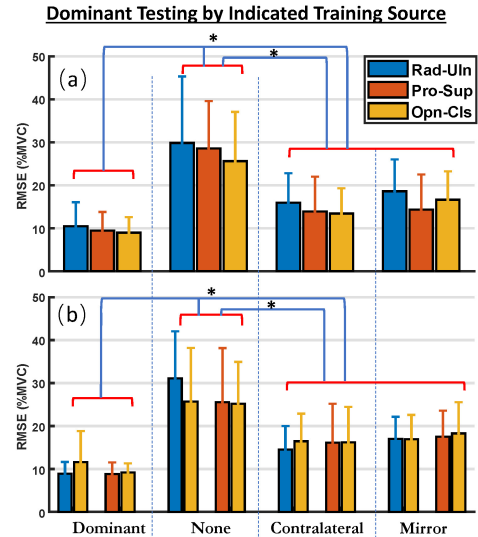


Fig. 5. Mean \pm std. dev. EMG-force RMSEs when testing on forces from the dominant limbs of able-bodied subjects and training from indicated feedback source [dominant force (Task 1), target with no visual feedback (Task 2), contralateral force (Task 3), target during mirror visual feedback (Task 3)], for (a) 1-DoF and (b) 2-DoF tasks. EMG acquired from the dominant limb. Statistically significant differences between feedback types indicated with “*”.

C. Train EMG-Force, EMG-Target: Test Using Dominant Limb Forces of Able-Bodied Subjects (Tasks 1–3)

Fig. 5 shows summary results of EMG-force/target models trained with the various indicated signal as the supervised output, but always tested using a distinct trial of able-bodied dominant limb forces. Thus, regardless as to whether the training set used force or target as the output, the model was tested using dominant limb force as the output. When training did not use dominant limb force, then testing on the dominant limb best indicates if the supervised output is an acceptable surrogate for dominant limb force—which, of course, is not available in limb-absent subjects. Note that training with dominant force feedback (same side as the electrode array) represents the best-case EMG-force training condition (EMG recorded directly from muscles producing the measured force/moment).

In 1-DoF tasks, a two-way RANOVA with factors: DoF (Rad-Uln, Pro-Sup, Opn-Cls) and feedback (dominant, contralateral, none, mirror) found only feedback was significant [$F(1.3, 14) = 45, p_{GG} = 10^{-6}$]. Post hoc comparison found that dominant feedback had significantly lower RMSE than the others ($p < 0.002$), contralateral and mirror had no significant difference from each other, and both had lower RMSE than none ($p < 0.001$).

In 2-DoF tasks, a three-way RANOVA with factors: DoF pair (Rad-Uln & Opn-Cls, Pro-Sup & Opn-Cls), feedback (dominant, contralateral, none, mirror) and motion-within-DoF (wrist Rad-Uln vs. hand Opn-Cls, or wrist Pro-Sup vs. hand Opn-Cls) found only feedback was significant [$F(1.4, 16) = 37, p_{GG} = 10^{-6}$]. Pairwise comparison found that dominant feedback had significantly lower RMSE than

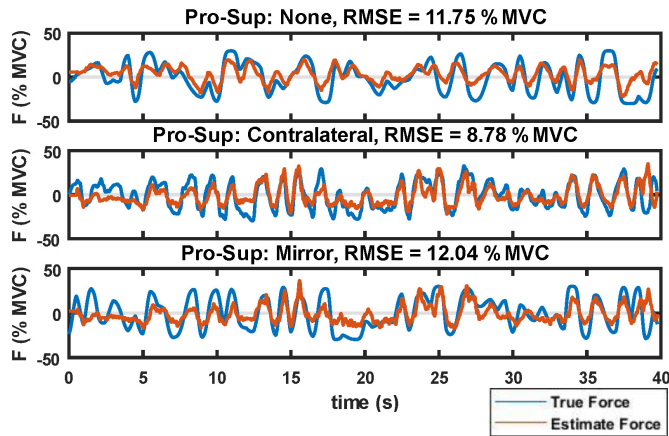


Fig. 6. Example 1-DoF EMG-force/target time-series results, limb-absent subject 22, Pro-Sup, for three feedbacks (none, contralateral force, mirror). EMG acquired from the affected side. Both true force and EMG-estimated force are shown in each plot.

the others ($p < 0.001$), contralateral and mirror had no significant difference from each other, and both had lower RMSE than none ($p < 0.004$).

D. Train EMG-Force, EMG-Target: Test Using Respective Feedback Signal—All Subjects (Tasks 2, 3)

Fig. 6 and Fig. 7 show example time-series results.² Fig. 8 shows summary results of EMG-force/target models when the distinct train and test trials were from the *same* feedback signal *other* than dominant force. These three signals were available for both able-bodied and limb-absent subjects, so provide a more direct means of comparison between these subject populations which is not available from the prior results.

In 1-DoF tasks, a three-way RANOVA for RMSE with two subject-within factors: feedback (contralateral, none, mirror) and DoF (Rad-Uln, Pro-Sup, Opn-Cls); and one subject-between factor: group (able-bodied, limb-absent) found significant interactions. Thus, two-way RANOVAs were computed separately for able-bodied and limb-absent subjects. For able-bodied subjects, the two-way RANOVA found only feedback was significant [$F(2, 22) = 12.5, p = 10^{-4}$]. Pairwise comparison showed that contralateral feedback had significantly lower error than none ($p = 0.04$) and mirror ($p = 10^{-4}$). For limb-absent subjects, the two-way RANOVA found both feedback and DoF significant [$F(2, 22) > 4.0, p < 0.05$]. Pairwise comparison showed that contralateral feedback had significantly lower error than none ($p = 0.035$) and mirror ($p = 0.015$), and that Pro-Sup had better performance than Rad-Uln ($p = 0.021$). Alternatively, we fixed each of the DoFs in the original three-way RANOVA. Of these three two-way RANOVAs, only when Rad-Uln was fixed was a significant difference found in the group factor, with able-bodied subjects exhibiting lower error than limb-absent [$F(1, 17) = 10.8, p = 0.004$].

²Note that there is sufficient subject-to-subject variation that finding one trial with each RMSE near its average result is not feasible. Thus, the rank order of the RMSEs shown in these figures does not necessarily follow those of the summary results.

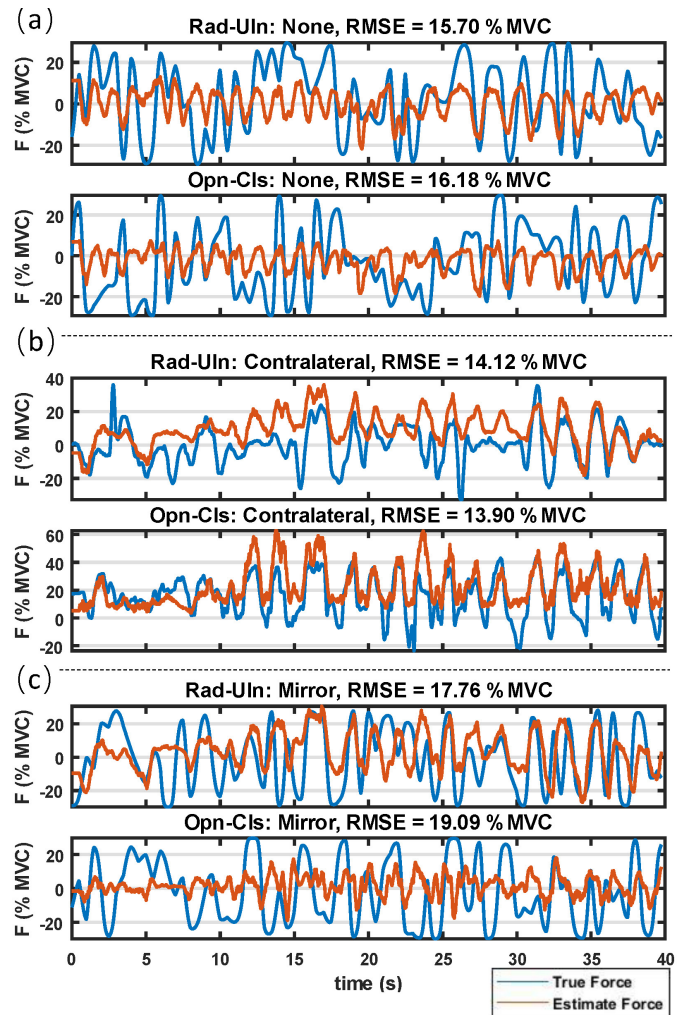


Fig. 7. Example 2-DoF EMG-force time-series results, limb-absent subject 21, Rad-Uln & Opn-Cls when using (a) no feedback, (b) contralateral feedback and (c) mirror feedback. EMG acquired from the affected side. Both true force and EMG-estimated force are shown in each plot.

In 2-DoF tasks, a four-way RANOVA for RMSE with three subject-within factors: feedback (contralateral, none, mirror), DoF pair (Rad-Uln & Opn-Cls; Pro-Sup & Opn-Cls) and motion-within-DoF (wrist Rad-Uln vs. hand Opn-Cls, or wrist Pro-Sup vs. hand Opn-Cls); and a subject-between factor: group (able-bodied, limb-absent) found DoF to not be significant [$F(1, 17) = 0.3, p = 0.6$], and the other three factors to interact. Continuing analysis of the three interacting factors, two three-way RANOVAs with factor group fixed were computed. For able-bodied subjects, there was a two-way significant interaction of feedback \times motion-within-DoF. Thus, pairwise comparison found that: for both motion-within-DoF wrist Rad-Uln and Pro-Sup, contralateral feedback had significantly lower RMSE than mirror ($p = 0.008$); for motion-within-DoF hand Opn-Cls, contralateral feedback exhibited significantly lower RMSE than both none ($p < 10^{-4}$) and mirror ($p = 0.001$). For limb-absent subjects, the three-way RANOVA found only feedback significant [$F(1.1, 6.4) = 9.4, p = 0.02$]. Pairwise comparison found contralateral feedback had significant lower RMSE than mirror ($p = 0.033$).

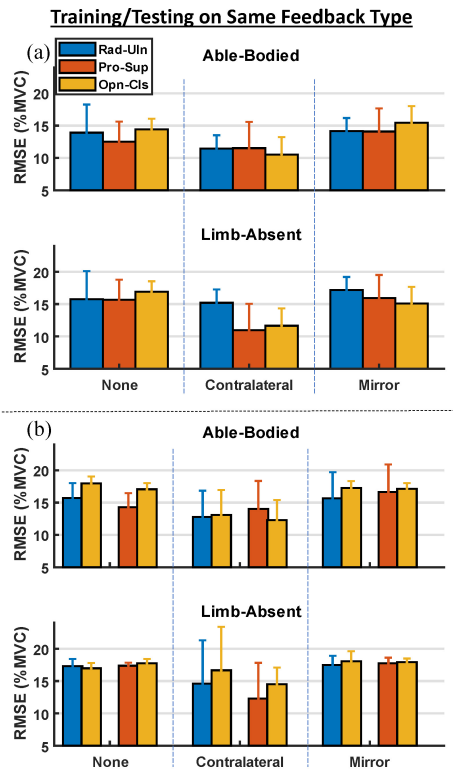


Fig. 8. (a) 1-DoF mean \pm std. dev. EMG-force/target RMSEs when testing and training on trials from the same feedback type [none (Task 2), contralateral force (Task 3), mirror (Task 3)] three motion pairs for both able-bodied and limb-absent subjects. (b) Corresponding 2-DoF RMSE results. EMG acquired from the dominant limb of able-bodied subjects, affected side of limb-absent subjects. Statistically significant differences described in text.

IV. DISCUSSION

A. Latencies Between Force/Moment and Target

The 1-DoF latencies between force/moment and target (Table II) are generally consistent with those found in the literature, ranging in average from 234–367 ms [42]. When tracking using the contralateral (i.e., non-dominant) limb of able-bodied subjects for feedback, the latencies tended to be longer.

Latencies for our 2-DoF tasks were not readily found within the literature, hence our results for these tasks may be novel. Across Tasks 1–3, the trend was for much larger average latencies (by a factor of ~ 2) for the Opn-Cls dimension within each 2-DoF task, while the other contraction dimension retained a latency similar to its 1-DoF task. Standard deviations were similar to the 1-DoF results. The only exception was Rad-Uln & Opn-Cls 2-DoF Task 2—in this case both constituent DoFs exhibited the higher average latencies. Anecdotal observation during the trials suggests that subjects struggled to perform the 2-DoF tracking, and may have concentrated their tracking focus on Rad-Uln/Pro-Sup at the expense of Opn-Cls. Additionally, use of arrowhead size as the feedback source for Opn-Cls may have been more challenging compared to the other DoFs. But, this issue is less likely, since no similar performance distinction occurred in 1-DoF. Note that in able-bodied subjects, each subject’s latency was available,

thus these subject-specific latencies provided the most accurate estimates. For limb-absent subjects, we resorted to using the average value from able-bodied subject trials from the same task and DoF. This approximation was necessary, but likely contributed more error to the limb-absent results.

B. RMSE, Dominant Force vs. Target, Able-Bodied Subjects

The results in Fig. 4 depict the ability of forces/moments in the dominant arm of able-bodied subjects to track the target, as a function of three feedback sources. As expected, when dominant feedback is provided from the dominant limb, errors are statistically lower. Our results then show a hierarchy of performance, with mirror feedback showing the next lowest error and no-feedback providing the highest error. These results are consistent both for 1- and 2-DoF tasks. Notably, the error between the target and the actual force produced by the dominant arm in the no-feedback condition averaged 25–30 %MVC, even though the full force range only spanned ± 30 %MVC. Hence, this error was nearly half the available force range, which is quite large; suggesting that the target displayed during the no-feedback condition is quite a poor supervised output source for system identification purposes.

In contrast, the maximum cross-correlation results for all of these tasks are quite high (Fig. 4, right). The average value of ρ ranged from ~ 0.6 to over 0.8 for the 1-DoF tasks. As shown in the time-series plots of Fig. 6 and Fig. 7, subjects followed the *timing* of the extrema of target force quite well, but had difficulty in maintaining proper amplitude (especially for 2-DoF tasks).

C. Train EMG-Force, EMG-Target: Test Using Dominant Limb Forces of Able-Bodied Subjects

Fig. 5 shows the principal results of this study. Relating EMG from the dominant limb to forces in that limb, as expected, gives EMG-force models with the lowest errors—since EMG is recorded directly from the muscles producing the measured force/moment. The errors found herein are consistent in magnitude with those found in prior studies [44], [45]. It is also encouraging that the EMG-force errors shown in Fig. 5 are similar in amplitude to the force tracking errors shown in Fig. 4. Thus, relating EMG to dominant side force has errors that are similar to those between dominant force and the target. But, when dominant limb forces are not available and a surrogate output is needed to train EMG-force for the dominant limb (e.g., limb-absent subjects), our results again found a hierarchy of statistically significant differences: bilateral tracking using contralateral force for training (with or without mirror visual feedback) performed somewhat poorer, while no feedback performed the poorest. Statistically, there was no performance distinction in bilateral tracking between feedback of contralateral force and mirror visual feedback. For both 1- and 2-DoF tasks, the EMG-force/target errors with no feedback were approximately half the available force range. These errors are so large that it is likely that population-based models of EMG-force dynamics (e.g., Hill-style muscle models [46] or generic EMG-force calibrations from a

population [30], [31]), combined with estimation only of one gain parameter per EMG channel, would provide considerably better EMG-force estimation. For example, in a 2-DoF hand-wrist EMG-force task involving nine able-bodied subjects [31], we replaced EMG-force dynamics calibrated to each individual with one universal model calibrated across the population. A single gain per EMG channel was still optimally estimated per individual. The population-based model performed nearly identically to those customized to each individual. Of course, optimal gain selection still requires force estimation from the dominant limb. However, prosthetists are familiar with the subtleties of EMG channel gain selection.

Note that EMG-force calibration using contralateral force feedback (with or without mirror feedback) still requires use of a load cell. This option might be reasonable for use in a prosthetist's office, but does not seem reasonable for field calibration of a prosthesis control system.

D. Train EMG-Force, EMG-Target: Test Using Respective Feedback Signal—All Subjects

Finally, Fig. 6 and Fig. 7 show results when EMG-force/target models were trained and tested from the same signal source, excluding the previously shown Task 1 results from training using dominant limb force. These models importantly highlight results from the limb-absent subjects (whose anatomy does not permit measurement of affected-side limb forces). The associated statistical results are not as sharply defined, perhaps reflecting the larger result variances and the smaller sample size. Nonetheless, there was still a general trend for lower errors when training EMG-force/target models using contralateral feedback, and unacceptably higher errors when training with no feedback—consistent with results from the able-bodied subjects. Also, there were limited distinctions between the wrist DoFs (although Pro-Sup did have better 1-DoF performance than Rad-Uln). Pro-Sup would be the most intuitive if used to control wrist rotation. And, in limb-absent subjects, it is interesting to note that providing mirror visual feedback was not statistically different from providing no feedback.

E. General Discussion and Limitations

Our results found a rather clear performance hierarchy, with dominant limb feedback providing the lowest EMG-force error (as would be expected), followed by feedback based on bilateral tracking (using either the forces from the contralateral side, or mirror visual tracking), followed by no feedback. EMG-force models based on bilateral tracking seemed adequate, but require the use of a load cell and would exclude persons with bilateral limb-absence. EMG-target models formed using no feedback seemed inadequate. In such cases, population-based EMG-force models (as least for EMG-force dynamics; one gain per EMG channel is always needed to scale its contribution) might perform better.

In general, we chose to equate the dominant side of able-bodied subjects to the affected side of limb-absent subjects. We did so because prostheses aspire to be a high quality replacement of limb function (which is best represented by

the dominant side in able-bodied subjects) and, thus, we wish to advance prosthesis control towards the performance expectations of the dominant limb. In addition, most prior EMG-force modeling has been performed on the dominant side of able-bodied subjects. Nevertheless, the sound side of limb-absent subjects becomes used as the dominant side, regardless of natural handedness—due largely to the limited functionality provided by existing prostheses.

We did not find many substantive differences in performance as a function of DoF. Such changes have been found in the literature (e.g., when relating dominant-limb EMG to hand position in the contralateral hand of able-bodied subjects, during bilateral mirror contractions [36]) and postulated to be consistent with deeper muscle fibers (which are more poorly represented in surface EMG) that are prime torque generators for the poorer performing DoFs [47]. Perhaps if such differences exist, they are subtle enough to be difficult to find with the small sample sizes common in experimental studies in this field. Also, the use of a large number of electrodes, placed about the full extent of the remnant limb (as was done in our work), may help to mitigate these issues [36].

The tasks tested in this study were relatively novel to both our able-bodied and limb-absent subjects. In particular, 2-DoF target tracking was both novel and challenging. It would be interesting to determine if more tracking practice (or, repeated experimental sessions) would have led to better 2-DoF tracking [48], [49]. Note that our force-varying target trajectories were selected for their system identification properties (uniform distribution gives equal weight to each force level; bandlimited and white gives equal weight to each frequency). If subjects are better able to produce the requested forces, the quality of the identified model is likely to improve.

We separated our statistical analyses of 1-DoF tasks from those of 2-DoF tasks, because these tasks are inherently different. Testing for a statistical difference between inherently distinct tasks is, generally, not of scientific value [16], [44]. As shown in Table II, Opn-Cls tracking latencies during 2-DoF tasks trended longer than those from 1-DoF tasks. Similarly, Fig. 5 and Fig. 8 suggest a trend for larger 2-DoF EMG-force RMSEs compared to 1-DoF. These trends are consistent with our anecdotal observation that subjects had more difficulty tracking in 2-DoFs than 1-DoF. Future work might seek to better understand the decrement in performance, if any, in 2-DoF tracking tasks vs. 1-DoF tracking tasks.

It is always important to recognize that the neuromuscular anatomy of limb-absent subjects is both different from that of able-bodied subjects and highly variable. For example, our able-bodied subjects had a mean \pm std. dev. forearm circumference of 25.9 ± 3.2 cm compared to 22.2 ± 2.3 cm for the limb-absent subjects. Remnant muscle tissue typically has more neuromuscular damage and may be more prone to fatigue (e.g., [48]). And, the sensation of a phantom hand may be more or less expressive in different subjects. Anecdotally, phantom limb sensation may have been more of a limitation in 2-DoF tasks than in 1-DoF tasks. Each of these factors may influence EMG-force performance.

Finally, there is some evidence suggesting that an accurate model of the dynamics between muscular activation (inputs)

and kinetic/kinematic outputs is *not* paramount to control of the existing generation of myoelectrically-controlled prostheses, which provide relatively rudimentary function. If the myoelectric control model is repeatable and largely linear, then prosthesis users are hypothesized to adapt/re-learn the necessary inputs (muscular activations) required to achieve the desired output [48], [50], [51]. In fact, existing commercial prosthesis users have been doing so for years, albeit at the cost of additional mental workload (among other limiting factors) [52]. Of course, the higher the fidelity with which future prosthetic devices reproduce the function of intact limbs, the more apparent will become the benefit of accurately identifying models relating muscular activation to kinetics/kinematics. And, unilateral prosthesis users should benefit from more accurate forward-path activation models during, for example, bilaterally symmetric tasks, wherein the central nervous system nominally matches muscular activation between the affected and the sound side.

V. CONCLUSION

The prime goal of this work was to evaluate distinct options for surrogate supervised output sources in hand-wrist EMG-force models for limb-absent subjects. We did so using novel instrumentation in which hand Opn-Cls forces as well as wrist Rad-Uln force and Pro-Sup moment were simultaneously measured on both sides of our able-bodied subjects. This instrumentation allowed us to report novel quantitative results on the latency between force/moment and our random target (Table II); and on the ability of these subjects to perform random target tracking during our various tasks, contrasting RMSE to cross-correlation coefficient (Fig. 4).

For EMG-force modeling, our comparison of different feedback approaches found that use of the phantom limb for bilateral tracking (with or without mirror visual feedback) permitted the limb on the sound side to provide a reasonable substitute force measurement. But, this output source is only available to persons with unilateral limb-absence and still requires use of a load cell. As such, it is primarily of use in a prosthetist's office, and not in the field. We found that use of the tracking target without a feedback source (applicable to limb-absent subjects) resulted in an inadequate EMG-force model. In such cases, use of generic models for EMG-force dynamics, combined with simple gain selection for each EMG channel, would likely provide better performance.

REFERENCES

- [1] V. S. Ramachandran and D. Rogers-Ramachandran, "Synaesthesia in phantom limbs induced with mirrors," *Proc. R. Soc. London B*, vol. 263, no. 1369, pp. 377–386, 1996.
- [2] K. T. Reilly, "Persistent hand motor commands in the amputees' brain," *Brain*, vol. 129, no. 8, pp. 2211–2223, Jul. 2006.
- [3] P. Parker, K. Englehart, and B. Hudgins, "Myoelectric signal processing for control of powered limb prostheses," *J. Electromyogr. Kinesiol.*, vol. 16, no. 6, pp. 541–548, Dec. 2006.
- [4] R. W. Mann, "Cybernetic limb prosthesis: The ALZA distinguished lecture," *Ann. Biomed. Eng.*, vol. 9, no. 1, pp. 1–43, Jan. 1981.
- [5] B. Hudgins, P. Parker, and R. N. Scott, "A new strategy for multifunction myoelectric control," *IEEE Trans. Biomed. Eng.*, vol. 40, no. 1, pp. 82–94, Jan. 1993.
- [6] T. A. Kuiken *et al.*, "Targeted muscle reinnervation for real-time myoelectric control of multifunction artificial arms," *J. Amer. Med. Assoc.*, vol. 301, pp. 619–628, Feb. 2009.
- [7] J. M. Hahne, M. A. Wilke, M. Koppe, D. Farina, and A. F. Schilling, "Longitudinal case study of regression-based hand prosthesis control in daily life," *Frontiers Neurosci.*, vol. 14, p. 600, Jun. 2020.
- [8] N. Jiang, K. B. Englehart, and P. A. Parker, "Extracting simultaneous and proportional neural control information for multiple-DOF prostheses from the surface electromyographic signal," *IEEE Trans. Biomed. Eng.*, vol. 56, no. 4, pp. 1070–1080, Apr. 2009.
- [9] T. S. Buchanan, D. G. Lloyd, K. Manal, and T. F. Besier, "Neuromusculoskeletal modeling: Estimation of muscle forces and joint moments and movements from measurements of neural command," *J. Appl. Biomechanics*, vol. 20, no. 4, pp. 367–395, Nov. 2004.
- [10] D. Staudenmann, K. Roeleveld, D. F. Stegeman, and J. H. van Dieën, "Methodological aspects of SEMG recordings for force estimation—A tutorial and review," *J. Electromyogr. Kinesiol.*, vol. 20, no. 3, pp. 375–387, Jun. 2010.
- [11] E. A. Clancy, L. Liu, P. Liu, and D. V. Z. Moyer, "Identification of constant-posture EMG-Torque relationship about the elbow using nonlinear dynamic models," *IEEE Trans. Biomed. Eng.*, vol. 59, no. 1, pp. 205–212, Jan. 2012.
- [12] P. Liu, L. Liu, and E. A. Clancy, "Influence of joint angle on EMG-torque model during constant-posture, torque-varying contractions," *IEEE Trans. Neural Syst. Rehabil. Eng.*, vol. 23, no. 6, pp. 1039–1046, Nov. 2015.
- [13] C. J. Abul-Haj and N. Hogen, "Functional assessment of control systems for cybernetic elbow prostheses. I. description of the technique," *IEEE Trans. Biomed. Eng.*, vol. 37, no. 11, pp. 1025–1036, Nov. 1990.
- [14] M. A. Golkar, E. Sobhani Tehrani, and R. E. Kearney, "Linear parameter varying identification of dynamic joint stiffness during time-varying voluntary contractions," *Frontiers Comput. Neurosci.*, vol. 11, p. 35, May 2017.
- [15] T. Kawase, H. Kambara, and Y. Koike, "A power assist device based on joint equilibrium point estimation from EMG signals," *J. Robot. Mechatron.*, vol. 24, no. 1, pp. 205–218, Feb. 2012.
- [16] C. Dai, Z. Zhu, C. Martinez-Luna, T. R. Hunt, T. R. Farrell, and E. A. Clancy, "Two degrees of freedom, dynamic, hand-wrist EMG-force using a minimum number of electrodes," *J. Electromyogr. Kinesiol.*, vol. 47, pp. 10–18, Aug. 2019.
- [17] R. A. Popat *et al.*, "Quantitative assessment of four men using above-elbow prosthetic control," *Arch. Phys. Med. Rehabil.*, vol. 74, no. 7, pp. 720–729, Jul. 1993.
- [18] N. Hogan and R. W. Mann, "Myoelectric signal processing: Optimal estimation applied to electromyography—Part I: Derivation of the optimal myoprocessor," *IEEE Trans. Biomed. Eng.*, vol. BME-27, no. 7, pp. 382–395, Jul. 1980.
- [19] E. A. Clancy and K. A. Farry, "Adaptive whitening of the electromyogram to improve amplitude estimation," *IEEE Trans. Biomed. Eng.*, vol. 47, no. 6, pp. 709–719, Jun. 2000.
- [20] C. Dai, B. Bardizbanian, and E. A. Clancy, "Comparison of constant-posture force-varying EMG-force dynamic models about the elbow," *IEEE Trans. Neural Syst. Rehabil. Eng.*, vol. 25, no. 9, pp. 1529–1538, Sep. 2017.
- [21] R. H. Messier, J. Duffy, H. M. Litchman, P. R. Paslay, J. F. Soechting, and P. A. Stewart, "The electromyogram as a measure of tension in the human biceps and triceps muscles," *Int. J. Mech. Sci.*, vol. 13, no. 7, pp. 585–598, Jul. 1971.
- [22] L. H. Smith, T. A. Kuiken, and L. J. Hargrove, "Evaluation of linear regression simultaneous myoelectric control using intramuscular EMG," *IEEE Trans. Biomed. Eng.*, vol. 63, no. 4, pp. 737–746, Apr. 2016.
- [23] A. Ameri, E. N. Kamavuako, E. J. Scheme, K. B. Englehart, and P. A. Parker, "Support vector regression for improved real-time, simultaneous myoelectric control," *IEEE Trans. Neural Syst. Rehabil. Eng.*, vol. 22, no. 6, pp. 1198–1209, Nov. 2014.
- [24] J. Vredenburg and G. Rau, "Surface electromyography in relation to force, muscle length and endurance," *New Develop. Electromyogr. Clin. Neurophysiol.*, vol. 1, pp. 607–622, 1973.
- [25] J.-J. Luh, G.-C. Chang, C.-K. Cheng, J.-S. Lai, and T.-S. Kuo, "Isokinetic elbow joint torques estimation from surface EMG and joint kinematic data: Using an artificial neural network model," *J. Electromyogr. Kinesiol.*, vol. 9, no. 3, pp. 173–183, Apr. 1999.
- [26] M. M. Liu, W. Herzog, and H. H. C. M. Savelberg, "Dynamic muscle force predictions from EMG: An artificial neural network approach," *J. Electromyogr. Kinesiol.*, vol. 9, no. 6, pp. 391–400, Dec. 1999.

- [27] J. Hashemi, E. Morin, P. Mousavi, K. Mountjoy, and K. Hashtrudi-Zaad, "EMG-force modeling using parallel cascade identification," *J. Electromyogr. Kinesiol.*, vol. 22, pp. 469–477, Jun. 2012.
- [28] N. Jiang, H. Rehbaum, I. Vujaklija, B. Graimann, and D. Farina, "Intuitive, online, simultaneous, and proportional myoelectric control over two degrees-of-freedom in upper limb amputees," *IEEE Trans. Neural Syst. Rehabil. Eng.*, vol. 22, no. 3, pp. 501–510, May 2014.
- [29] C. Lin, B. Wang, N. Jiang, and D. Farina, "Robust extraction of basis functions for simultaneous and proportional myoelectric control via sparse non-negative matrix factorization," *J. Neural Eng.*, vol. 15, no. 2, Apr. 2018, Art. no. 026017.
- [30] L. Pan, D. L. Crouch, and H. Huang, "Myoelectric control based on a generic musculoskeletal model: Toward a multi-user neural-machine interface," *IEEE Trans. Neural Syst. Rehabil. Eng.*, vol. 26, no. 7, pp. 1435–1442, Jul. 2018.
- [31] B. Bardizbanian *et al.*, "Efficiently training two-DoF hand-wrist EMG-force models," in *Proc. 42nd Annu. Int. Conf. IEEE Eng. Med. Biol. Soc. (EMBC)*, Montreal, QC, Canada, Jul. 2020, pp. 369–373.
- [32] D. A. Winter, *Biomechanics and Motor Control of Human Movement*. Hoboken, NJ, USA: Wiley, 2009, pp. 250–280.
- [33] K. Koirala, M. Dasog, P. Liu, and E. A. Clancy, "Using the electromyogram to anticipate torques about the elbow," *IEEE Trans. Neural Syst. Rehabil. Eng.*, vol. 23, no. 3, pp. 396–402, May 2015.
- [34] J. L. G. Nielsen, S. Holmgaard, N. Jiang, K. B. Englehart, D. Farina, and P. A. Parker, "Simultaneous and proportional force estimation for multifunction myoelectric prostheses using mirrored bilateral training," *IEEE Trans. Biomed. Eng.*, vol. 58, no. 3, pp. 681–688, Mar. 2011.
- [35] S. Muceli, N. Jiang, and D. Farina, "Multichannel surface EMG based estimation of bilateral hand kinematics during movements at multiple degrees of freedom," in *Proc. Annu. Int. Conf. IEEE Eng. Med. Biol.*, Buenos Aires, Argentina, Aug. 2010, pp. 6066–6069.
- [36] S. Muceli and D. Farina, "Simultaneous and proportional estimation of hand kinematics from EMG during mirrored movements at multiple degrees-of-freedom," *IEEE Trans. Neural Syst. Rehabil. Eng.*, vol. 20, no. 3, pp. 371–378, May 2012.
- [37] C. Andison, "EMG-based assessment of active muscle stiffness and co-contraction in muscles with primary and secondary actions at the wrist during piano playing," M.S. thesis, Dept. Mech. Aero. Eng. Appl. Sci., Carleton Univ., Ontario, ON, Canada, 2011.
- [38] C. Mercier, "Mapping phantom movement representations in the motor cortex of amputees," *Brain*, vol. 129, no. 8, pp. 2202–2210, Jul. 2006.
- [39] B. L. Chan *et al.*, "Mirror therapy for phantom limb pain," *New England J. Med.*, vol. 357, no. 21, pp. 2206–2207, Nov. 2007.
- [40] N. Jiang, J. L. Vest-Nielsen, S. Muceli, and D. Farina, "EMG-based simultaneous and proportional estimation of wrist/hand kinematics in uni-lateral trans-radial amputees," *J. NeuroEng. Rehabil.*, vol. 9, no. 1, p. 42, 2012.
- [41] A. Ameri, E. J. Scheme, E. N. Kamavuako, K. B. Englehart, and P. A. Parker, "Real-time, simultaneous myoelectric control using force and position-based training paradigms," *IEEE Trans. Biomed. Eng.*, vol. 61, no. 2, pp. 279–287, Feb. 2014.
- [42] R. D. Luce, *Response Times: Their Role in Inferring Elementary Mental Organization*. Oxford, U.K.: Oxford Univ. Press, 1986, pp. 209–210.
- [43] M. Azaria and D. Hertz, "Time delay estimation by generalized cross correlation methods," *IEEE Trans. Acoust., Speech, Signal Process.*, vol. ASSP-32, no. 2, pp. 280–285, Apr. 1984.
- [44] E. A. Clancy, C. Martinez-Luna, M. Wartenberg, C. Dai, and T. R. Farrell, "Two degrees of freedom quasi-static EMG-force at the wrist using a minimum number of electrodes," *J. Electromyogr. Kinesiol.*, vol. 34, pp. 24–36, Jun. 2017.
- [45] B. Bardizbanian *et al.*, "Calibration of dynamic hand-wrist EMG-force models using a minimum number of electrodes," in *Proc. IEEE Signal Process. Med. Biol. Symp. (SPMB)*, Philadelphia, PA, USA, Dec. 2018, pp. 1–2.
- [46] A. L. Hof and J. Van den Berg, "EMG to force processing I: An electrical analogue of the hill muscle model," *J. Biomechanics*, vol. 14, no. 11, pp. 747–758, Jan. 1981.
- [47] A. M. Gilroy, B. R. MacPherson, L. M. Ross, J. Broman, and A. Josephson, *Atlas of Anatomy*. Berlin, Germany: Thieme, 2008, pp. 328–336.
- [48] J. M. Hahne, M. A. Schweisfurth, M. Koppe, and D. Farina, "Simultaneous control of multiple functions of bionic hand prostheses: Performance and robustness in end users," *Sci. Robot.*, vol. 3, no. 19, Jun. 2018, Art. no. eaat3630.
- [49] A. Tabor, S. Bateman, and E. Scheme, "Evaluation of myoelectric control learning using multi-session game-based training," *IEEE Trans. Neural Syst. Rehabil. Eng.*, vol. 26, no. 9, pp. 1680–1688, Sep. 2018.
- [50] J. M. Hahne, M. Markovic, and D. Farina, "User adaptation in myoelectric man-machine interfaces," *Sci. Rep.*, vol. 7, no. 1, p. 4437, Dec. 2017.
- [51] N. Jiang, I. Vujaklija, H. Rehbaum, B. Graimann, and D. Farina, "Is accurate mapping of EMG signals on kinematics needed for precise online myoelectric control?" *IEEE Trans. Neural Syst. Rehabil. Eng.*, vol. 22, no. 3, pp. 549–558, May 2014.
- [52] T. W. Williams, "Practical methods for controlling powered upper-limb prostheses," *Assistive Technol.*, vol. 2, no. 1, pp. 3–18, Mar. 1990.